An optical-optical double-resonance study of the Rydberg states of O-2. I. The ns and nd (gerade) states excited via single-rotational levels of the b (1)Sigma(+)(0g) valence state

An optical–optical double-resonance study of the Rydberg states of O2. I. The ns and nd (gerade) states excited via single-rotational levels of the b 1Σ0g+ valence state

Howard A. Sheard, Trevor Ridley, Kenneth P. Lawley, and Robert J. Donovan

Citation: J. Chem. Phys. **118**, 8781 (2003); doi: 10.1063/1.1566948
View online: http://dx.doi.org/10.1063/1.1566948
View Table of Contents: http://jcp.aip.org/resource/1/JCPSA6/v118/i19
Published by the AIP Publishing LLC.

An optical–optical double-resonance study of the Rydberg states of O_2. I. The *ns* and *nd* (*gerade*) states excited via single-rotational levels of the $b\,^1\Sigma_{0g}^+$ valence state

Howard A. Sheard, Trevor Ridley,[a] Kenneth P. Lawley, and Robert J. Donovan
School of Chemistry, The University of Edinburgh, West Mains Road, Edinburgh, EH9 3JJ, Scotland, United Kingdom

(Received 4 November 2002; accepted 21 February 2003)

The ns ($n=4-9$) and nd ($n=3-8$) Rydberg states of O_2 converging on $O_2^+\ X\,^2\Pi_{1/2g}$ and $X\,^2\Pi_{3/2g}$ have been studied using optical–optical double resonance via single rotational levels of the initially excited $b\,^1\Sigma_{0g}^+$ valence state, together with multiphoton ionization. Both ns and nd states show a transition from (Λ,S) coupling to (Ω,ω) coupling as n increases. Transitions to all four components of an ns cluster are observed and rotational linestrengths show that the $ns\,^3\Pi_{2,1,0_g^+}\leftarrow\leftarrow b\,^1\Sigma_{0g}^+$ transitions borrow intensity from the $ns\,^1\Pi_{1g}\leftarrow\leftarrow b\,^1\Sigma_{0g}^+$ transition. © *2003 American Institute of Physics.* [DOI: 10.1063/1.1566948]

I. INTRODUCTION

The Rydberg states of O_2 have been studied by a variety of techniques. The $3s\,C\,^3\Pi_g$ and $3s\,d\,^1\Pi_{1g}$ Rydberg states have been investigated using (2+1) resonance-enhanced multiphoton ionization (REMPI), primarily from the $X\,^3\Sigma_g^-$ ground state,[1–5] although the $a\,^1\Delta_{2g}$ state (generated using a microwave discharge) has been used in later studies.[4,6] The $3s\,C\,^3\Pi_g$ state, which lies at lower energy than the $3s\,d\,^1\Pi_{1g}$ state, is a typical triplet state, having Ω components 0, 1, and 2 in order of increasing energy. Although all three Ω components were observed via (2+1) REMPI from the triplet $X\,^3\Sigma_g^-$ ground state, only $v=2$ of the $\Omega=1$ component was observed from the singlet $a\,^1\Delta_{2g}$ state due to spin–orbit interaction (~98% $^3\Pi_{1g}$, 2% $^1\Pi_{1g}$) with the two-photon allowed $3s\,d\,^1\Pi_{1g}$ state. The observed spectra show rich rotational structure that can only be partially resolved due to the relatively large linewidths produced by predissociation.

Some vibrational levels of $n=4$ and 5 of the ns Rydberg series have previously been observed using (2+1) REMPI from the ground state.[7,8] However, analysis of these spectra proved difficult partly because of the spectral congestion which arises from the number of J levels that are populated in the ground state, even in a molecular beam, and partly because of the large number of strong electronic transitions that are observed from the ground state. All of the previous experimental studies on the ns states have been reviewed in detail by Morrill *et al.*[9] They observed that the splittings between the four Ω components of the ns states indicate a transition from (Λ,S) coupling to (Ω,ω) coupling as n increases from 3 to 5 (see Sec. III below for further discussion).

The nd Rydberg states have also been widely investigated using (2+1) REMPI, from both the $X\,^3\Sigma_g^-$ and $a\,^1\Delta_{2g}$ states, and the results reviewed by Morrill.[10] It was concluded by Pratt *et al.*[11] that, like the ns states, the nd states undergo a transition from (Λ,S) coupling to (Ω,ω) coupling as n increases.

In previous publications,[12–14] we have reported the use of optical–optical double-resonance with REMPI (OODR/REMPI) to study the $v=0$, 1, and 3 levels of the $3s\,d\,^1\Pi_{1g}$ state excited via single rotational levels of the $b\,^1\Sigma_{0g}^+$ valence state. When $J=0$ of the $b\,^1\Sigma_{0g}^+$ state is pumped, a maximum of two J levels can be excited in each vibronic state via a two-photon transition. Thus the spectra are greatly simplified. In the present work, this OODR/REMPI excitation scheme is used to study higher-energy ns states with $n=4-9$ and also several nd states with $n=3-8$. In a companion paper,[15] the same technique is used to study some np and nf states via three-photon transitions from the $b\,^1\Sigma_{0g}^+$ state.

II. EXPERIMENT

The laser arrangement was comprised of two pulsed and independently tunable dye lasers (a Lambda Physik FL3002 and a Lambda Physik FL2002) pumped by a XeCl excimer laser (a Lambda Physik EMG201MSC). The fundamental output of R700 was used to pump the (0,0) band of the $b\leftarrow X$ transition around 760 nm. The frequency-doubled outputs of C102, C307, and C153 were used to generate the 235–285 nm probe photons. The wavelength of the probe laser was calibrated by simultaneously recording the neon optogalvanic spectrum to give an estimated accuracy in the two-photon energy of $\pm 0.5\ cm^{-1}$. In addition, there may be a small degree of power broadening of the peaks which will increase the error in the transition energy measurements. Also, some of the lines, e.g., those of the $4s$ states, have linewidths of around $5\ cm^{-1}$, resulting in a further increase in the error limits. Thus it is estimated that the experimental values quoted are accurate to $\pm 1\ cm^{-1}$; except for those of the $4s$ states which are only accurate to $\pm 2-3\ cm^{-1}$.

[a]Author to whom correspondence should be addressed. Fax: +44-131-6506453. Electronic mail: tr01@holyrood.ed.ac.uk

The counterpropagating pump and probe laser beams were focused to overlapping points in a differentially pumped ionization chamber using lenses of focal length 6 cm and intersected, at 90°, a pulsed molecular beam generated using a backing pressure of 600 torr of O_2. The resulting ions were ejected into a linear time-of-flight mass spectrometer, and the ion current from the microchannel plate detector was processed by a boxcar integrator and stored on a PC.

III. RESULTS AND DISCUSSION

A. Spectroscopic notation for the Rydberg states of O_2

Molecular Rydberg states can be described by both (Λ,S) and (Ω,ω) coupling schemes. The former has been shown to be most appropriate for the low-n Rydberg states of O_2, while the latter becomes more appropriate as n increases.

In (Λ,S), Hund's case (a) coupling, Λ, Σ, S, and Ω are all good quantum numbers. If the spin–orbit interaction is neglected, the energy differences between λ_{Ryd} components of each nl cluster are determined primarily by core-Rydberg Coulomb and exchange terms. For low-lying states, the (Λ,S) coupling is appropriate since the spin–orbit coupling constant A_c governing for the splitting between the $X\,^2\Pi_{3/2g}$ and $X\,^2\Pi_{1/2g}$ states of the ion core is much less than the exchange energy $K(1\pi_g:n\lambda_{\mathrm{Ry}})$. A much smaller contribution to the spin–orbit energy comes from the Rydberg electron.

The energy splittings due to the Coulomb and exchange interactions decrease as n^{-3}, while the spin–orbit coupling in the core remains effectively constant. Thus, in the limit of high n, the spin–orbit interaction completely mixes those Hund's case (a) basis states that involve linear combinations of the core spin–orbitals $[\pi_g^+]_c$ and $[\pi_g^-]_c$ associated with the two core spin–orbit states $X\,^2\Pi_{3/2}$ and $X\,^2\Pi_{1/2}$, so that Ω_c becomes a good quantum number. Ω is of course conserved during the mixing, though S is not, and the new coupling can be described as Hund's case (c). However, there are two additional quantum numbers that are good in the limit $A_c \gg K$, before the spin of the electron recouples to J at very high n. These are Ω_c, already discussed, and ω_{Ry} $(=|\lambda_{\mathrm{Ry}}+m_{s,\mathrm{Ry}}|)$ so that $\Omega=\Omega_c+\omega_{\mathrm{Ry}}$. This is (Ω,ω) coupling and the basis states that can be constructed from all possible combinations of Ω_c, λ_{Ry}, and $m_{s,\mathrm{Ry}}$ with λ_{Ry} ranging from 0 to 3 are listed in Table I. There is one unpaired electron in the core and one Rydberg electron, and if $m_{s,c}+m_{s,\mathrm{Ry}}=0$, then these states are linear combinations of equal weights of singlet- and triplet-spin states, denoted by $^{1+3}\Lambda$.

B. OODR technique

In the present paper an OODR scheme is used in which the low-lying $b\,^1\Sigma_{0g}^+$ state is used as intermediate state through rotationally selective optical pumping from the $X\,^3\Sigma_g^-$ ground state. The $b\,^1\Sigma_{0g}^+$ state is then probed to find coherent two-photon transitions to *gerade* Rydberg states, from which a further probe photon can ionize the molecule, i.e.,

TABLE I. Microconfigurations of the $nl\,^2\Pi_g$ Rydberg states with $\lambda_{\mathrm{Ry}}=0-3$ and their correlations with the (Ω,ω) and (Λ,S) coupling descriptions. In the micrconfigurations, $\pi\equiv\lambda_c=+1$ and $\underline{\pi}\equiv\lambda_c=-1$ and the $\pm$ superscripts indicate $m_s=\pm1/2$ of the ionic core and Rydberg electron. The overall parity of the states is that of the Rydberg orbital selected, since the $^2\Pi$ core is *gerade*.

$\Omega_c=1/2$

Ω	$^{2S+1}\Lambda$	Microconfiguration $[\pi_g m_s]_c(\lambda m_s)_{\mathrm{Ry}}$
4	$^{1+3}\Gamma$	$[\pi^-]3^+$
3	$^3\Gamma$	$[\pi^-]3^-$
3	$^{1+3}\Phi$	$[\pi^-]2^+$
2	$^3\Phi$	$[\pi^-]2^-$
2	$^{1+3}\Delta$	$[\pi^-]1^+$
1	$^3\Delta$	$[\pi^-]1^-$
1	$^{1+3}\Pi$	$[\pi^-]0^+$
$0^\pm$	$^3\Pi$	$2^{-1/2}([\pi^-]0^-\pm[\underline{\pi}^+]0^+)$
$0^\pm$	$^{1+3}\Sigma^\pm$	$2^{-1/2}([\pi^-]\underline{1}^+\pm[\underline{\pi}^+]1^-)$
1	$^3\Sigma$	$[\underline{\pi}^+]1^+$
1	$^{1+3}\Pi$	$[\underline{\pi}^+]2^-$
2	$^3\Pi$	$[\underline{\pi}^+]2^+$
2	$^{1+3}\Delta$	$[\underline{\pi}^+]3^-$
3	$^3\Delta$	$[\underline{\pi}^+]3^+$

$\Omega_c=3/2$

Ω	$^{2S+1}\Lambda$	Microconfiguration $[\pi_g]_c(\lambda m_s)_{\mathrm{Ry}}$
5	$^3\Gamma$	$[\pi^+]3^+$
4	$^{1+3}\Gamma$	$[\pi^+]3^-$
4	$^3\Phi$	$[\pi^+]2^+$
3	$^{1+3}\Phi$	$[\pi^+]2^-$
3	$^3\Delta$	$[\pi^+]1^+$
2	$^{1+3}\Delta$	$[\pi^+]1^-$
2	$^3\Pi$	$[\pi^+]0^+$
1	$^{1+3}\Pi$	$[\pi^+]0^-$
1	$^3\Sigma$	$[\pi^+]\underline{1}^+$
$0^\pm$	$^{1+3}\Sigma^\pm$	$2^{-1/2}([\pi^+]\underline{1}^-\pm[\pi^-]1^+)$
$0^\pm$	$^3\Pi$	$2^{-1/2}([\pi^+]\underline{2}^+\pm[\underline{\pi}^-]2^-)$
1	$^{1+3}\Pi$	$[\underline{\pi}^-]2^-$
1	$^3\Delta$	$[\underline{\pi}^-]3^-$
2	$^{1+3}\Delta$	$[\underline{\pi}^-]3^-$

$$O_2^+ \leftarrow {}'\text{Rydberg state} \leftarrow {}' \leftarrow {}' b\,^1\Sigma_{0g}^+(v=0,\ J=0) \leftarrow X\,^3\Sigma_g^-.$$

We designate this excitation-ionization scheme $(1+[(2')+1'])$, where the prime refers to a probe photon and the inner parentheses emphasize the coherent two-photon nature of the Rydberg$\leftarrow b$ transition. In a companion paper, OODR schemes in which coherent three-photon transitions from the $b\,^1\Sigma_{0g}^+$ state are applied—i.e., $(1+[(3')+1'])$ when three probe photons are used and $(1+[(2'+1)+1'])$ when two probe and one pump photons are used.

One of the major advantages of the OODR technique is that, due to the simplified nature of the resulting spectra, underlying states or structure that would normally be obscured by dense rotational structure become observable. A good illustration of this effect is shown in Fig. 1. Figure 1(a) shows the (2+1) REMPI spectrum in the region of $v=1$ of the $3d$ Rydberg states excited from the ground state and is similar to the spectrum of the $v=0$ states recorded by Glab *et al.*[16] Figure 1(b) shows the same energy region excited by $1+[(2')+1']$ OODR/REMPI, via $J=0$, $v=0$ of the $b\,^1\Sigma_{0g}^+$

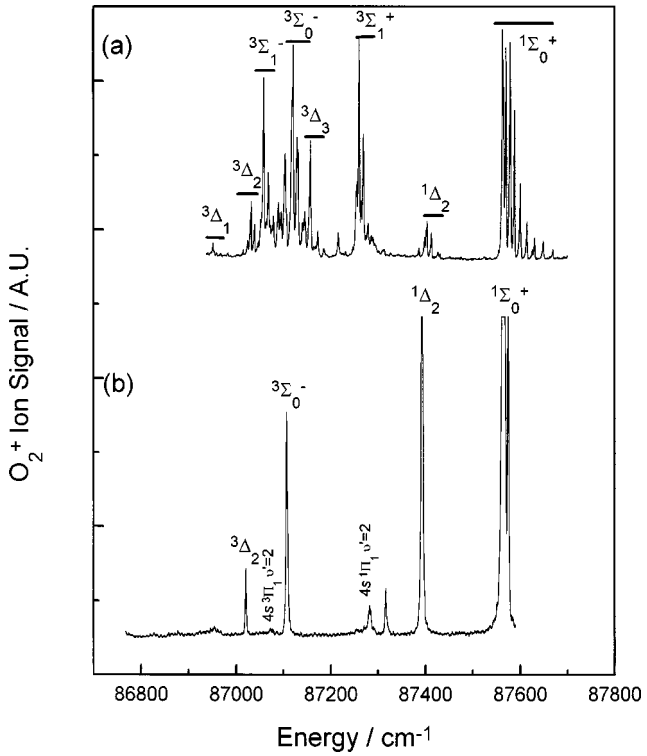

FIG. 1. (a) (2+1) REMPI spectrum of $v=1$ of the $3d$ complex of O_2 excited from the $X\,^3\Sigma_g^-$ ground state. The extent of the rotational envelope of each state is indicated by the dark lines. (b) $(1+[(2')+1'])$ OODR/REMPI spectrum recorded via $v=0$, $J=0$ of the $b\,^1\Sigma_{0g}^+$ valence state. The single peaks in the two $4s$ states and the $3d\,^{1,3}\Delta_{2g}$ states are S branches, that in the $3d\,^3\Sigma_{0g}^-$ state is a Q branch, and the double peak in the $3d\,^1\Sigma_{0g}^+$ state is comprised of a strong, off-scale Q branch and a weaker S branch. The weak unlabeled peak at 87 313 cm^{-1} may be due to one of the $3d\,^1\Pi_{1g}$ states.

valence state. At most, two rotational lines in each of the electronic states are observed in the OODR spectrum. This contrasts with the many rotational lines seen in each of the eight $3d$ states observed in the spectrum in Fig. 1(a). Thus it was possible to observe weaker structure, identified as $v=2$ of the $4s\,^1\Pi_{1g}$ and $4s\,^3\Pi_{1g}$ states, which is obscured by the overlapping dense rotational structure of the $3d$ states in the (2+1) REMPI spectrum [Fig. 1(a)].

One further advantage of the OODR technique is that when a single rotational level is pumped at the intermediate stage, the observed lines can be unambiguously identified, their positions accurately measured, and their intensities obtained. This approach has already been used to study the $3s\,d\,^1\Pi_{1g}$ state[12–14] and is used here to investigate the $5s$ states.

OODR can also help in the measurement of rotational linewidths, particularly of predissociated levels. There are two factors that make it difficult to accurately measure the widths of lines in conventional spectra that are significantly broadened by predissociation. First, there is the problem of the increased overlap of lines which means that it is not always possible to identify single rotational lines that are overlapped by others. The OODR technique effectively circumvents this problem. It does little, however, to alleviate the second problem: namely, that higher laser powers are usually required to ionize predissociated states, and hence the lines are weaker and there is an increased chance of power broadening.

One of the advantages of OODR also gives rise to one of its disadvantages. Since, at most, only five rotational lines in any upper state can be excited in two-photon transitions from a single-rotational level of the lower state, only information on those five levels can be obtained in a single spectrum. With the exception of the rotational analysis of some $5s$ states, in which various single-rotational levels in the $b\,^1\Sigma_{0g}^+$ state were pumped in turn, only $J=0$ of the $b\,^1\Sigma_{0g}^+$ was used in the present experiments. The choice of $J=0$ in the lower state, while simplifying the spectra even more (at most, only two rotational lines in any upper state can be excited in two-photon transitions), also further limits the amount of information, e.g., concerning J-dependent coupling, which can be gained about each of the upper states. Thus care must be taken not to draw conclusions about an entire excited state on the basis of observations of the characteristics of one or two rotational levels.

C. General overview of the OODR/REMPI spectrum

The spectra shown in Fig. 1 give a very good illustration of the different oscillator strengths for transitions from the $X\,^3\Sigma_g^-$ and $b\,^1\Sigma_{0g}^+$ states to the Rydberg states. A similar comparison of the oscillator strengths for transitions from the $X\,^3\Sigma_g^-$ and $a\,^1\Delta_{2g}$ states is shown in Fig. 3 of Ogorzalek-Loo *et al.*[4] The observed intensities can be rationalized from a consideration of the spin of the states involved. In the $b\,^1\Sigma_{0g}^+$ state the spins of the two open-shell π_g electrons are strongly coupled to form a singlet state (as are the electrons in the $a\,^1\Delta_{2g}$ state). Of the $24\,nd$ Rydberg states (22 if splitting of the two $^3\Pi_{0g}$ states into $^3\Pi_{0g^+}$ and $^3\Pi_{0g^-}$ substates is ignored), only six—$^1\Sigma_{0g}^+$, $^1\Sigma_{0g}^-$, $^1\Pi_{1g}(\times 2)$, $^1\Delta_{2g}$, and $^1\Phi_{3g}$—are singlet states in (Λ,S) coupling. Thus, if spin is to be conserved, only two-photon transitions from $b\,^1\Sigma_{0g}^+$ to the $^1\Sigma_{0g}^+$, $^1\Pi_{1g}$, and $^1\Delta_{2g}$ states are allowed.

However, while transitions to four states are seen in the spectrum in Fig. 1(b), only those to the $^1\Sigma_{0g}^+$ and $^1\Delta_{2g}$ are expected in Hund's case (a) (the $^1\Pi_{1g}$ states are not observed strongly). The other two weaker transitions, to the $^3\Sigma_{0g}^-$ and $^3\Delta_{2g}$ states, are observed because spin–orbit coupling in the core mixes the $^3\Sigma_{0g}^-/^1\Sigma_{0g}^+$ and $^3\Delta_{2g}/^1\Delta_{2g}$ states. Nevertheless, the spin eigenfunction of the mixed states can always be resolved into the singlet and triplet components, and the $S=0$ component carries the oscillator strength in transitions from either the $b\,^1\Sigma_{0g}^+$ or $a\,^1\Delta_{2g}$ states. Transitions to the $^1\Phi_{3g}$ state, forbidden in the $b\,^1\Sigma_{0g}^+$ spectrum, are seen strongly in the $a\,^1\Delta_{2g}$ state spectrum.[4,17]

The two $^1\Pi_{1g}$ ($3d\sigma_g$ and $3d\delta_g$) components are not seen strongly. It is possible, however, that the weak peak at 87 313 cm^{-1} in Fig. 1(b) is due to one of the $^1\Pi_{1g}$ components. Predissociation is one of several reasons why the two $3d\,^1\Pi_{1g}$ states are not observed, and this will be discussed briefly in Sec. III F.

As n increases, spin–orbit coupling in the core becomes dominant and in the limit of high n each pair of spin–orbit coupled components, $^{1,3}\Lambda$, are separated by the spin–orbit splitting of the ground state of the ion (200 cm^{-1}). At this

limit both components are a 50/50 mixture of the singlet and triplet states defined in Hund's case (a) and spectra to these mixed states from any lower-energy state should have similar intensities. The (2+1) REMPI spectrum of the 85 000–99 000 cm^{-1} energy region, i.e., up to and slightly above the first ionization energy (IE) of 97 348 cm^{-1},[18] excited from the ground state has been reported previously.[4,7,11,17,19–22] It was shown by Pratt *et al.*[11] that the spectrum of the *nd* series for $n \geqslant 5$ becomes very simple. Only the higher-*n* members of the $^3\Sigma_{0g}^-/^1\Sigma_{0g}^+$ coupled pair are observed. These levels can be clearly correlated with levels of a particular O_2^+ ion core state, and this seems to confirm that the Rydberg states become more accurately described by (Ω,ω) coupling as *n* increases. Higher members $(n \geqslant 5)$ of the $nd\ ^{1,3}\Delta_g$ states are not observed.

An overview of the 85 000–99 000 cm^{-1} energy region recorded by OODR/REMPI via $J=0$, $v=0$ of the $b\ ^1\Sigma_{0g}^+$ state is shown in Fig. 2. As the figure is a composite of ten spectra, none of which are power normalized, only a broad overview of the relative intensities of the peaks can be ob-

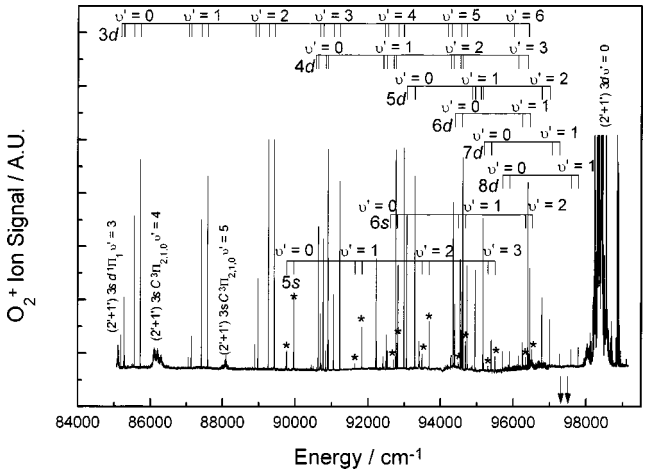

FIG. 2. Overview of the 85 000–99 000 cm^{-1} energy region of the $(1+[(2')+1'])$ OODR/REMPI spectrum of O_2 recorded via $v=0$, $J=0$ of the $b\ ^1\Sigma_{0g}^+$ state. The 5*s* and 6*s* states are starred. Several broad one-color, probe-laser-only peaks are labeled. The IEs of $O_2^+\ X\ ^2\Pi_{1/2g}$ and $X\ ^2\Pi_{3/2g}$ of 97 348 and 97 548 cm^{-1}, respectively, are arrowed.

TABLE II. Experimental (upper) and literature (lower) term values of the lowest rotational levels ($J=\Omega$), in cm^{-1} and the effective quantum numbers (n^*) of $v=0$, calculated using ionization energies of $O_2^+\ X\ ^2\Pi_{1/2g}$ and $X\ ^2\Pi_{3/2g}$ of 97 348 and 97 548 cm^{-1}, respectively (Refs. 18 and 23), of some *nd* (*gerade*) Rydberg states of O_2. The experimental values are relative to a zero in the $X\ ^3\Sigma_g^-$ ground state defined by Slanger and Cosby (Ref. 24).

			v						
State	*n*	*n**	0	1	2	3	4	5	6
$^3\Delta_{2g}$	3	3.00	85154.2	87020.0	88856.6	90659.1	92428.0	94167.3	
			85152.6[a]	87020.6[a]	88856.2[a]	90659.1[a]	92428.0[a]		
$^3\Sigma_{0g}^-$	3	3.01	85245.7	87106.6	88943.4	90742.5	92507.5	94243.7	95945.4
			85243.8[a]	87109.6[a]	88942.2[a]	90742.0[a]	92508.8[a]		
$^1\Delta_{2g}$	3	3.02	85524.9	87390.5	89228.9	91029.9	92797.9	94533.0	
			85523.7[a]	87392.1[a]	89226.3[a]	91028.3[a]			
$^1\Sigma_{0g}^+$	3	3.04	85691.5	87559.6	89395.2	91197.3	92967.4	94699.0	96405.0
			85690.5[a]	87558.6[a]	89394.3[a]	91196.8[a]			
$^3\Delta_{2g}$	4	4.02	90552.7	92422.6	94260.0	96061.0			
$^3\Sigma_{0g}^-$	4	4.03	90605.8	92476.1	94314.3	96117.4			
			90605.5[a]	92476.1[a]					
$^1\Delta_{2g}$	4	4.03	90804.3	92675.6	94512.0	96316.4			
$^1\Sigma_{0g}^+$	4	4.05	90870.8	92741.2	94577.7	96383.0			
			90870.4[a]	92741.0[a]					
$^3\Sigma_{0g}^-$	5	5.05	93042.3	94914.8	96754.6				
			93042.8[b]	94914.0[b]	96752.7[b]				
$^1\Sigma_{0g}^+$	5	5.06	93262.5	95134.5	96969.9				
			93261.4[b]	95133.7[b]	96971.7[b]				
$^3\Sigma_{0g}^-$	6	6.06	94360.0	96233.0					
			94349.1[b]	96232.5[b]	98072.3[b]				
$^1\Sigma_{0g}^+$	6	6.06	94564.0	96428.2					
			94554.0[b]	96437.5[b]	98277.1[b]				
$^3\Sigma_{0g}^-$	7	7.08	95155.5	97026.3					
			95154.8[b]	97026.4[b]					
$^1\Sigma_{0g}^+$	7	7.08	95356.2	97228.1					
			95355.7[b]						
$^3\Sigma_{0g}^-$	8	8.09	95669.2	97544.4					
			95669.7[b]	97543.5[b]					
$^3\Sigma_{0g}^-$	8	8.09	95869.9	97742.6					
			95869.3[b]	97742.1[b]					

[a]Reference 7. The values quoted here are 1.3 cm^{-1} higher than those given in the literature in order to show them relative to the same zero in the $X\ ^3\Sigma_g^-$ ground state. See text for further details.

[b]Reference 11. These values are the transition energies of the most intense line as reported.

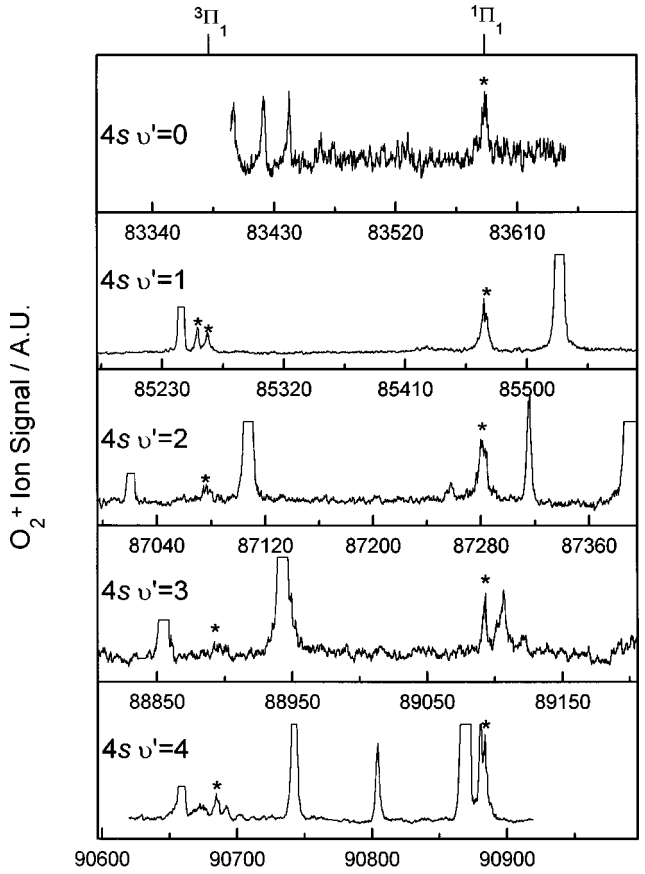

FIG. 3. (1+[(2′)+1′]) OODR/REMPI spectra of the 4*s* Rydberg states of O_2 (starred) recorded via $v=0$, $J=0$ of the $b\,^1\Sigma_{0g}^+$ state. The unlabeled, stronger, signals are due to *nd* states as observed in Fig. 2. The $^3\Pi_{1g}$ and $^1\Pi_{1g}$ markers are separated by 200 cm^{-1}.

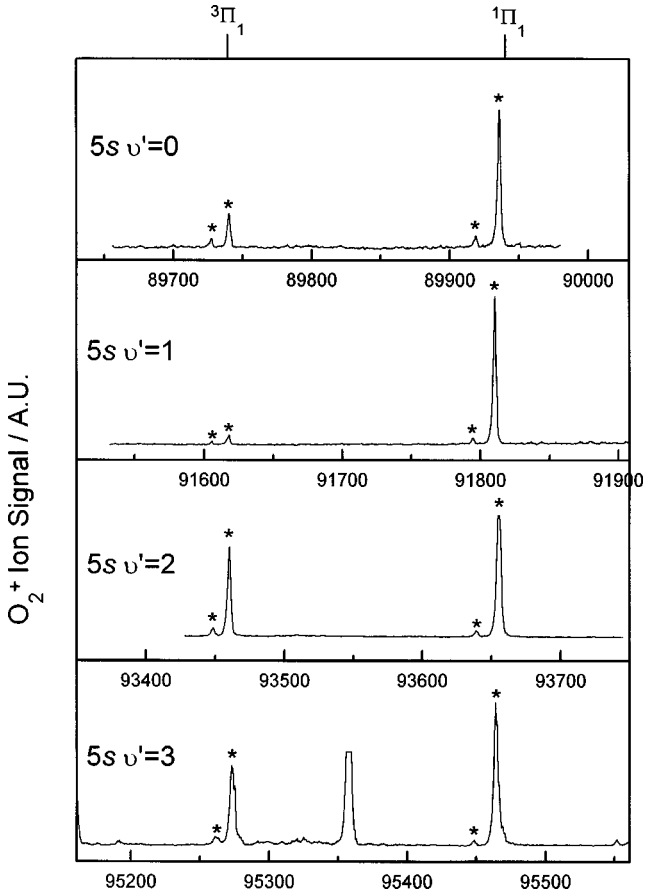

FIG. 4. (1+[(2′)+1′]) OODR/REMPI spectra of the 5*s* Rydberg states of O_2 (starred) recorded via $v=0$, $J=0$ of the $b\,^1\Sigma_{0g}^+$ state. The unlabeled, stronger, signals are due to *nd* states as observed in Fig. 2. See text for discussion of intensities.

tained. In particular, very strong transitions to some of the 3*d* and 4*d* states may be partially saturated.

The *ns* and *nd* states were identified mainly on the basis of their effective quantum number $n^*=(n-\delta)$, as calculated from the Rydberg equation,

$$T([\Omega_c]nl)=\mathrm{IE}(\Omega_c)-R/[n-\delta(l)]^2,$$

where $T([\Omega_c]nl)$ is the term value of the electronic state origin, R is the Rydberg constant (10 9735.5 cm^{-1}), δ is the quantum defect, and $\mathrm{IE}(\Omega_c)$ is the ionization energy of the spin–orbit component of the ion to which the Rydberg series converges. IEs of O_2^+ $X\,^2\Pi_{1/2g}$ and $X\,^2\Pi_{3/2g}$ of 97 348 cm^{-1} and 97 548 cm^{-1}, respectively, were used.[18,23] δ was found to be 1.20 ± 0.03 and -0.04 ± 0.04 for the *ns* and *nd* states, respectively. These agree closely with the values of 1.20 ± 0.05 and 0.03 ± 0.01 for the *ns* and *nd* states of atomic oxygen.

The spectrum is dominated by *nd* states having $n=3-8$. The *ns* states with $n=4$, 5, 6, 7, and 9 are also observed, although only those where $n=5$ and 6 are indicated in Fig. 2. The other *ns* states are too weak to be seen with the intensity scale used for Fig. 2, but are shown in expanded form in Figs. 3–6 (see below). Several one-color, probe-only (2+1) REMPI signals from the ground state of O_2 are also observed in Fig. 2 and are assigned to transitions to 3*s* and 3*d* states as shown. It is fortuitous that the range of probe laser energies, required to record the OODR/REMPI spectra reported here, lies in a window between these transitions.

D. *nd* states

The term values of the $nd\,^3\Sigma_{0g}^-$, $^1\Sigma_{0g}^+$, $^3\Delta_{2g}$, and $^1\Delta_{2g}$ states obtained from the spectra in Fig. 2 are presented in Table II. These, like all of the experimental term values presented here, are measured relative to the zero-point energy in the $X\,^3\Sigma_g^-$ ground state defined by Slanger and Cosby.[24] In each case, the values refer to the lowest possible rotational states ($J=\Omega$) and are accurate to approximately ±1 cm^{-1}. Also shown are one set of literature values for those states which have been seen previously.[7,11] There is some ambiguity about the 3*d* and 4*d* literature values referenced.[7] The authors claim that the values they presented correspond to the energy of the rotationless level of the state. However, from comparisons of these values with the results reported by the same group in an earlier paper[22] and with the present experimental values it appears that they probably refer to $J=\Omega$. Here 1.3 cm^{-1} has been added to the literature values in order to place them relative to the same value for zero in the $X\,^3\Sigma_g^-$ state that is used for the experimental values. The $(5-8)d$ literature values[11] refer to the strongest line in the spectrum.

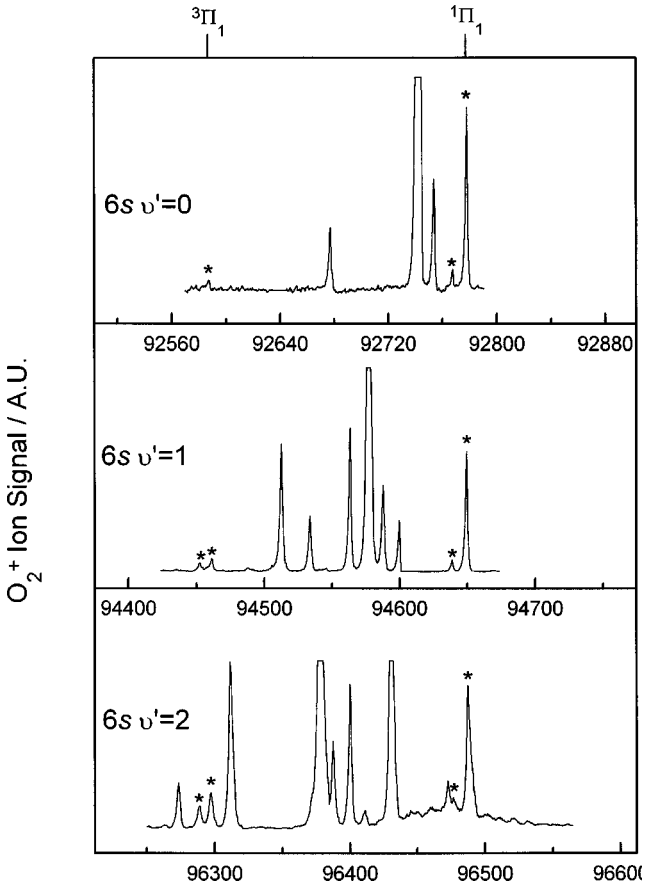

FIG. 5. (1+[(2′)+1′]) OODR/REMPI spectra of the 6*s* Rydberg states of O_2 (starred) recorded via $v=0$, $J=0$ of the $b\,^1\Sigma_{0g}^+$ state. The unlabeled, stronger, signals are due to *nd* states as observed in Fig. 2.

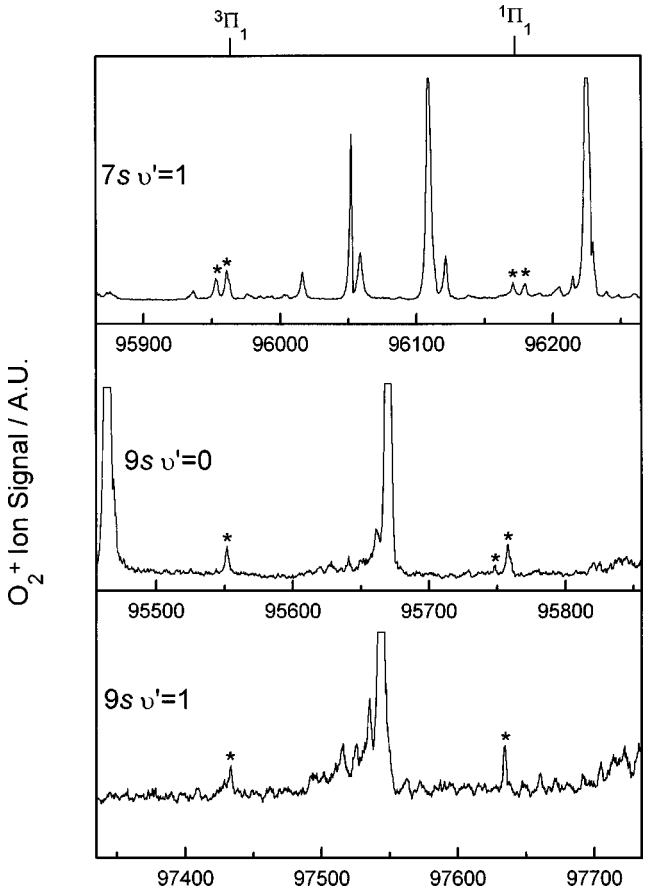

FIG. 6. (1+[(2′)+1′]) OODR/REMPI spectra of the 7*s* and 9*s* Rydberg states of O_2 (starred), recorded via $v=0$, $J=0$ of the $b\,^1\Sigma_{0g}^+$ state. The unlabeled, stronger, signals are due to *nd* states as observed in Fig. 2.

There are only two obvious discrepancies between the experimental and literature values. The present data show that the $v=0$ levels of the $6d\,^3\Sigma_{0g}^-/^1\Sigma_{0g}^+$ pair of states are ~ 10 cm^{-1} higher than reported in the literature.[11]

There are some observed lines remaining which cannot be assigned to transitions to the $nd\,^1\Sigma_{0g}^+$, $^1\Delta_{2g}$, $^3\Sigma_{0g}^-$, $^3\Delta_{2g}$, or *ns* states. It is believed that some of these unassigned lines are due to transitions to $na\,^1\Pi_{1g}$ states. However, the intensities of these lines, in any proposed vibrational progression, are very irregular and their assignments are much more speculative and will not be presented here.

E. *ns* states

Figures 3–6 show the *ns* states ($n=4$, 5, 6, 7, and 9) in greater detail. The unlabeled signals are due to *nd* states, as shown in Fig. 2. While these *ns* states should strictly be labeled according to the (Ω,ω) coupling scheme, the (Λ,S) coupling labels, appropriate for the 3*s* states, are retained for convenience.

On the basis of the calculated n^* values, several vibrational levels of the *ns* states for $n=4-9$ are identified. Previously, only $v=0-4$ of the 4*s* cluster and $v=0-1$ of the 5*s* cluster had been reported.[7,9] In the present work, the 7*s* ($v=0$) and 8*s* ($v=0,1$) could still not be observed due to overlapping *nd* structure. The 4*s* states are very weak compared to the higher-*ns* states as a result of predissociation (predissociated states are generally more difficult to detect in ionization experiments). The lower component of the 4*s* ($v=0$) pair is not observed as it is overlapped by one-color signals from the ground state.

It proved to be difficult to obtain reliable intensity measurements of the peaks in the spectra shown in Figs. 4–6, and it is estimated that the errors may be up to $\pm 30\%$. It is clear, however, that $v=1$ of the $5s\,^3\Pi_{1g}$ state is anomalously weak relative to $v=0$, 2, and 3, an observation for which we have no explanation.

The term values for the observed *ns* states, corresponding to $J=2$, are presented in Table III. Several of these vibronic levels have previously been rotationally analyzed.[7,9] The literature term values for the nonexistent $J=0$ of these rotationally analyzed levels (as before, increased by 1.3 cm^{-1} in order to place them relative to the same value for zero in the $X\,^3\Sigma_g^-$ state that is used for the experimental values) are also shown in Table III, for comparison. The $J=2$ to $J=0$ separation should be ~ 10 cm^{-1} assuming a B value of 1.7 cm^{-1} and is consistent with the average separation for the four 5*s* ($v=0$) levels, for which a comparison can be made. Since the remaining literature values for other vibronic levels either have large uncertainties attached to them or correspond to unassigned rotational lines, they are also consistent with the present experimental values.

The 5*s* states will be considered in more detail. It can be

TABLE III. Experimental (upper) term values of the $J=2$ rotational levels, in cm^{-1}, and the effective quantum numbers (n^*) of $v=0$, calculated using ionization energies of O_2^+ $X\ ^2\Pi_{1/2g}$ and $X\ ^2\Pi_{3/2g}$ of 97 348 and 97 548 cm^{-1}, respectively (Refs. 18 and 23), of some ns (*gerade*) Rydberg states of O_2. The literature (lower) values are taken from various experimental data, summarized by Morrill *et al.* (Ref. 9). In the literature, for $n=4$, the two different Ω states sharing a common core are not resolved.

			v				
State	n	n^*	0	1	2	3	4
$^3\Pi_{0+}$	3	1.86					
			65573[a]		69366[a]	71189[a]	
$^3\Pi_1$	3	1.86					
			65664[a]	67580[a]	69445[a]	71265[a]	72990[a]
$^3\Pi_2$	3	1.86					
			65767[a]		69550[a]	71375[a]	
$^1\Pi_1$	3	1.88					
			66361.4[13,b]	68234.3[14,b]	70016.7[b,c]	71952.4[12,b]	
$^3\Pi_{0+}$	4	2.80		85256.2			
			83346.2[d]	85250[a,e]	87090[a,e]	88890[a,e]	90649.8[d]
$^3\Pi_1$	4	2.80		85264.9	87075.8	88898.3	90684
			83373.0[d]	85250[a,e]	87090[a,e]	88890[a,e]	
$^3\Pi_2$	4	2.80					
			83536.2[d]	85420[a,e]	87260[a,e]	89070[a,e]	90834.5[d]
$^1\Pi_1$	4	2.80	83586.4	85468.8	87280.7	89094.5	90885.1
			83578[a]	85420[a,e]	87260[a,e]	89070[a,e]	
$^3\Pi_{0+}$	5	3.79	89727.8	91602.0	93447.9	95261.4	
			89719.7[d]	91621[a]			
$^3\Pi_1$	5	3.80	89740.4	91617.5	93459.8	95272.6	
			89728.8[d]	91615[a]			
$^3\Pi_2$	5	3.79	89918.7	91796.8	93639.2	95448.6	
			89908.3[d]	91798[a]			
$^1\Pi_1$	5	3.80	89935.3	91811.6	93655.1	95463.7	
			89925.0[d]	91809[a]			
$^3\Pi_{0+}$	6	4.80		94451.7	96289.5		
$^3\Pi_1$	6	4.80	92588.2	94460.8	96298.3		
$^3\Pi_2$	6	4.79	92766.4	94639.1	96476.4		
$^1\Pi_1$	6	4.80	92777.6	94649.9	96487.2		
$^3\Pi_{0+}$	7	5.80		95961.3			
$^3\Pi_1$	7	5.81		95969.5			
$^3\Pi_2$	7	5.81		96171.7			
$^1\Pi_1$	7	5.82		96180.5			
$^3\Pi_1$	9	7.82	95552.8	97433.7			
$^3\Pi_2$	9	7.81	95747.6				
$^1\Pi_1$	9	7.83	95756.8	97633.5			

[a]Transition energy of the strongest feature.
[b]Value for $J=1$.
[c]Unpublished results.
[d]Value for the nonexistent $J=0$ level derived from a rotational analysis (Refs. 7 and 9) and increased by 1.3 cm^{-1}.
[e]Uncertainty ± 20 cm^{-1}.

seen in Fig. 4 that $v=0-3$ of the $5s$ cluster consist of two closely spaced doublets separated by ~ 200 cm^{-1}, the ion–core splitting, the weaker partner in the doublets being to lower energy by $\sim 9-12$ cm^{-1}. Excitation of $v=0$ and 1 of the $5s$ states from the ground state has been reported by Yokelson *et al.*[7] They also observed four electronic states at each vibrational level which they assigned as the $^3\Pi_{0g^+}$, $^3\Pi_{1g}$, $^3\Pi_{2g}$, and $^1\Pi_{1g}$ components, in ascending order of energy. In contrast to our spectra, the lower energy of the two states with a common ionic core carried the most intensity. This is a consequence of the predominantly triplet $^3\Pi_{0g^+}$ and $^3\Pi_{2g}$ states being excited by a favorable transition from the triplet ground state. The $^3\Pi_{1g}$ and $^1\Pi_{1g}$ components, as a result of spin–orbit coupling in the core, have mixed singlet and triplet character and hence are seen more weakly. In excitation from the singlet $b\ ^1\Sigma_{0g}^+$ state, the reverse is true; the mixed states are seen more strongly.

Evidence for a similar coupling between the $3d\ ^1\Phi_{3g}$ and $3d\ ^3\Phi_g$ states was derived from the $(2+1)$ REMPI spectra excited from the $a\ ^1\Delta_{2g}$ state.[17] Strong transitions were observed to the $^1\Phi_{3g}$ and $^3\Phi_{3g}$ components which are coupled by a spin–orbit interaction in the core. The two states are seen with similar intensities and are separated by the spin–orbit splitting in the ground state of the ion. In addition, two weak components $^3\Phi_{2g}$ and $^3\Phi_{4g}$ were observed ~ 4 cm^{-1} to low energy of the $^1\Phi_{3g}$ and $^3\Phi_{3g}$ components, respectively.

In both cases, it was proposed[7,17] that the rotational energy levels of the $^3\Pi_{1g}$ and $^1\Pi_{1g}$ and $^3\Phi_{2g}$ and $^3\Phi_{3g}$ states

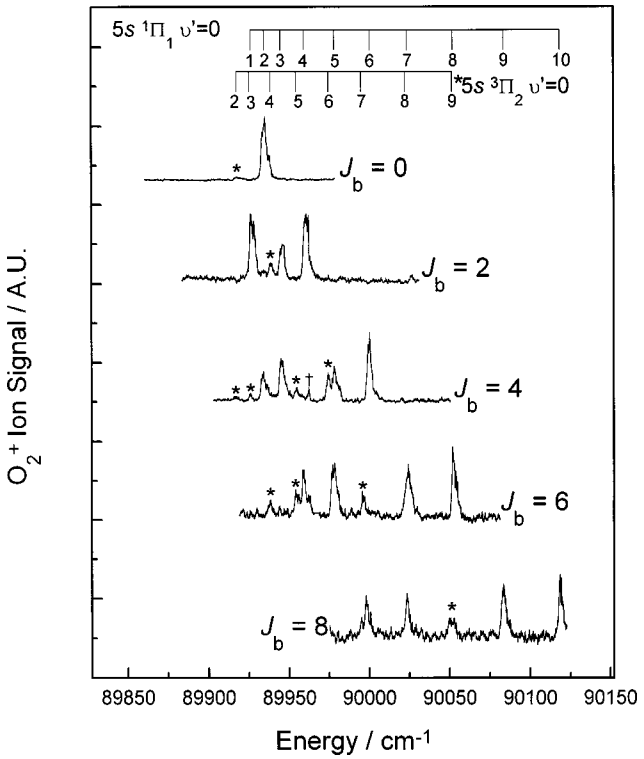

FIG. 7. (1+[(2′)+1′]) OODR/REMPI spectrum of $v'=0$ of the $5s\ ^3\Pi_{2g}$ (starred) and $5s\ ^1\Pi_{1g}$ (unlabeled) states of O_2 recorded via various rotational levels of the $b\ ^1\Sigma_{0g}^+$ state. Peaks labeled † are unassigned peaks. The ladders show the rotational energy levels of the Rydberg states.

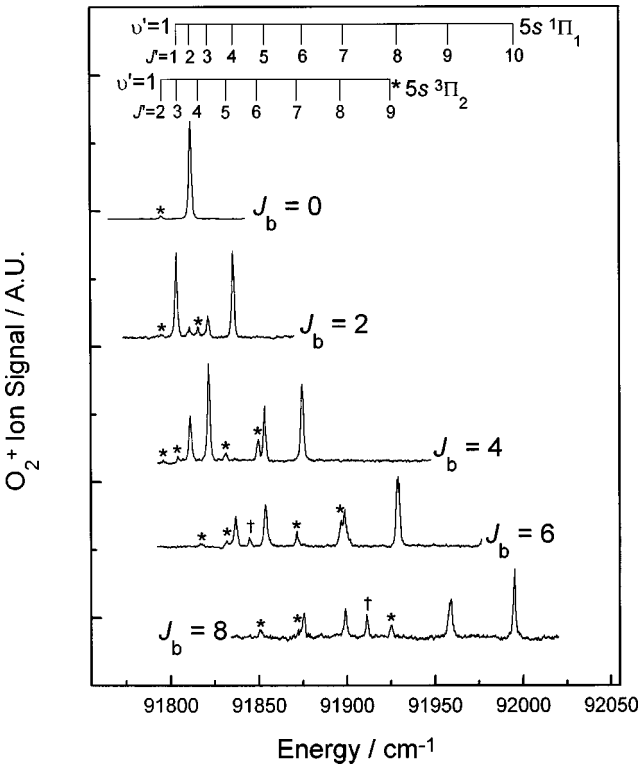

FIG. 8. (1+[(2′)+1′]) OODR/REMPI spectrum of $v'=1$ of the $5s\ ^3\Pi_{2g}$ (starred) and $5s\ ^1\Pi_{1g}$ (unlabeled) states of O_2 recorded via various rotational levels of the $b\ ^1\Sigma_{0g}^+$ state. Peaks labeled † are unassigned peaks. The ladders show the rotational energy levels of the Rydberg states.

TABLE IV. Rotational-branch energies, in cm^{-1}, for two-photon transitions to several vibronic levels of the $5s$ Rydberg states from $b\ ^1\Sigma_{0g}^+(v=0,J)$ observed in the OODR/REMPI spectrum of O_2.

$^1\Pi_1$ ($v=0$) J	$O(J)$	$P(J)$	$R(J)$	$S(J)$
0	⋯	⋯	⋯	76813.3
2	⋯	76796.4	76815.0	76830.0
4	76784.3	76795.6	76828.5	76851.5
6	76779.5	76798.1	76844.1	76872.1
8	76778.6	76802.0	76862.0	76896.9
$^3\Pi_2$ ($v=0$)				
0	⋯	⋯	⋯	76796.6
2	⋯	⋯	⋯	76809.4
4	76768.5	76777.2	76805.7	76825.9
6	76758.8	76774.8	76815.9	⋯
8	⋯	⋯	76830.8	⋯
$^1\Pi_1$ ($v=1$)				
0	⋯	⋯	⋯	78689.4
2	⋯	78673.9	78691.7	78705.8
4	78661.4	78672.2	78704.1	78724.9
6	78655.8	78673.4	78719.3	78747.4
8	78652.9	78677.5	78737.3	78772.5
$^3\Pi_2$ ($v=1$)				
0	⋯	⋯	⋯	78674.6
2	⋯	⋯	⋯	78687.2
4	78646.3	78655.6	78683.1	78701.6
6	78636.4	78652.5	78692.8	78717.8
8	78628.9	78650.7	78704.3	⋯
$^3\Pi_1$ ($v=2$)[a]				
0	⋯	⋯	⋯	80337.6
2	⋯	80322.3	80340.5	80355.1
4	80309.7	80320.8	80352.9	80375.2
6	80305.0	80322.9	80368.0	80395.7
8	80302.8	80328.7	80385.1	80418.7

[a]See Fig. 1 of Ref. 13.

do not fit very well the usual expression $T+BJ(J+1)$ and that a better fit could be achieved using the expression $T+\gamma J+BJ(J+1)$. It was further concluded that this was indicative of S uncoupling.

In the current experiments, by varying the pump wavelength, it was possible to rotationally analyze both $v=0$ and 1 of the $^3\Pi_{2g}$ and $^1\Pi_{1g}$ components of the $5s$ state. Different J levels of the intermediate state were pumped and the resulting rotational levels for both components can clearly be observed in the spectra shown in Figs. 7 and 8. The unmarked peaks correspond to the $\Omega=1$ state, peaks marked with asterisks correspond to the $\Omega=2$ state, and peaks marked with daggers are unassigned.

The observed rotational-branch energies to $v=0$ and 1 of the $5s\ ^3\Pi_{2g}$ and $5s\ ^1\Pi_{1g}$ Rydberg states from $b\ ^1\Sigma_{0g}^+(v=0,J)$ are presented in Table IV. The term values for the J levels of these vibronic levels calculated from the transition energies are presented in Table V. In a previous paper,[13] the rotational levels of $v=2$ of the $^3\Pi_{1g}$ state were observed (see Fig. 1 of Ref. 13). The equivalent rotational-branch energies and term values are also included in Tables IV and V.

Using the assignments in Figs. 7 and 8, rotational con-

TABLE V. Term values, in cm^{-1}, for the J levels of several vibronic levels of the $5s$ Rydberg states of O_2.

J	$^1\Pi_1\,(v=0)$	$^3\Pi_2\,(v=0)$	$^1\Pi_1\,(v=1)$	$^3\Pi_2\,(v=1)$	$^3\Pi_1\,(v=2)$
0	⋯	⋯	⋯	⋯	⋯
1	89927.0	⋯	91804.5	⋯	93452.9
2	89935.5	89918.7	91811.6	91796.8	93459.8
3	89945.7	89927.3	91822.3	91805.7	93471.0
4	89960.4	89939.7	91836.4	91817.8	93485.7
5	89978.7	89955.6	91854.1	91833.2	93503.3
6	90001.3	89976.0	91875.3	91851.7	93525.2
7	90024.6	89996.6	91899.9	91873.5	93548.9
8	90052.8	⋯	91928.1	91898.5	93576.4
9	90084.4	90053.2	91959.7	91926.7	93607.5
10	90119.3	⋯	91994.9	⋯	93641.1

stants were calculated for $v=0$ and 1 of the $^3\Pi_{2g}$ and $^1\Pi_{1g}$ states using the expression $T+\gamma J+BJ(J+1)$, and these are presented in Table VI. The errors in B and γ are typically ± 0.03 and ± 0.3 cm^{-1}, respectively, and the experimental values are reproduced to less than ± 1 cm^{-1}. The rotational constants for $v=0$ of the $^3\Pi_{2g}$ and $^1\Pi_{1g}$ states are in reasonable agreement with the values of Yokelson *et al.*[25] However, a fit which was not significantly poorer could also be achieved using the conventional expression $T+BJ(J+1)$. The B values obtained from this expression are also shown in Table VI. Thus, while the two states are clearly coupled by some mechanism in order for the $^3\Pi_{2g}$ state to be seen at all, the present rotational analysis cannot confirm that it is by S uncoupling.

In previous (2+1) REMPI studies on the $3d\,^1\Phi_{3g}$ and $3d\,^3\Phi_g$ states,[17] the observed line strengths of the weaker $^3\Phi_{2g}$ and $^3\Phi_{4g}$ components both appear to be those of a $\Delta\Omega=1$ transition, i.e., $\Omega'=3$ in particular, the $^3\Phi_{2g}$ state has a strong P branch which is absent in a $\Delta\Omega=0$ transition. Furthermore, transitions to the $J=2$ level in the Rydberg state are not observed. Both observations point to the conclusion that the $^3\Phi_{2g}$ state carries no oscillator strength and is only seen because of its mixing with the $^3\Phi_{3g}$ state as the spin uncouples. Furthermore, the line strengths have the Hönl–London factors of the component of the coupled state that carries the oscillator strength even if it is only a minor component. Thus the Ω value of the major contributor to the mixed state—i.e., $\Omega=2$ in this example—does not define the observed Hönl–London factors.

The lines observed in the spectra shown in Figs. 7 and 8 exhibit similar intensity characteristics: As expected, the intensities of the rotational branches of the $\Omega=1$ component from a single-J level in the intermediate state are similar to those observed for $v=0$ of the $3s\,d\,^1\Pi_{1g}$ state[13] and follow the expected pattern for a two-photon $\Delta\Omega=1$ transition.[26] The observed relative intensities of the rotational branches of the $\Omega=2$ component are also essentially the same as those of the $\Omega=1$ component.

Thus, overall, it appears that $5s\,^1\Pi_{1g}$ and $5s\,^3\Pi_{1g}$ states are mixed by spin–orbit coupling in the core, followed by further interactions with the $^3\Pi_{0g^+}$ and $^3\Pi_{2g}$ states. Two strong and two weak transitions are observed to the four states, all of which have the line strengths of a $\Delta\Omega=1$ transition. These doublets are seen in most of the higher-ns spectra shown in Figs. 4–6. No unambiguous doubling of the 4s states can be identified in Fig. 3 as the signal-to-noise is much lower. The $4s\,^3\Pi_{0g^+}/^3\Pi_{1g}\,(v=1)$ doublet is anomalous, and it has been proposed that it may undergo a heterogeneous interaction with the close lying, sharp, $3d\,^3\Sigma^-_{0g}$ state.[7] The $4s\,^3\Pi_{2g}/^1\Pi_{1g}\,(v=4)$ doublet also appears to be involved in an interaction.

F. Predissociation of the *ns* states

The numerous REMPI studies of the $3s$ Rydberg states have been reviewed by Morrill *et al.*[9] The $3s\,C\,^3\Pi_g$ and $3s\,d\,^1\Pi_{1g}$ states interact with several valence states. All of the interstate interactions have been modeled by Lewis *et al.*[27] using a coupled Schrödinger equation (CSE) approach to the problem. The results of the modeling predicted that interaction of the bound Rydberg states with the repulsive valence states would result in an oscillatory broadening of the rotational lines: e.g., predicted linewidths for $J=1$ of $v=1$, 2, and 3 of the $3s\,C\,^3\Pi_g$ state were 150, 1.5, and 77

TABLE VI. Rotational constants, in cm^{-1}, of some ns Rydberg states of O_2. The literature values were reported by Morrill *et al.* (Ref. 9) and were taken from unpublished work of Yokelson *et al.* (Ref. 25) and were calculated using the expression $T+\gamma J+BJ(J+1)$.

State	v	B[a]	B	γ	B (Lit.)[b]	γ (Lit.)[b]
$^3\Pi_2$	0	1.60	1.71	−1.3	1.628	−0.58
$^1\Pi_1$	0	1.78	1.68	1.2	1.719	0.75
$^3\Pi_2$	1	1.55	1.61	−0.8		
$^1\Pi_1$	1	1.76	1.75	0.2		
$^3\Pi_1$	2	1.75	1.64	1.3		

[a]Calculated using the expression $T+BJ(J+1)$.
[b]References 9 and 25.

cm^{-1}, respectively. Experimental linewidths of several vibrational levels of both the $3s\,C\,^3\Pi_g$ and $3s\,d\,^1\Pi_{1g}$ have been reported.[1,3,5,28–30] The calculated linewidths reproduce the trends in the experimental values well.

The effect of these interactions on the linewidths of the higher-ns clusters has also been simulated by Morrill *et al.*[9] The predicted linewidths for $v=0-4$ of the $4s\,^3\Pi_{1g}$ state vary between 3.5 and 6.5 cm^{-1}, while those of the $4s\,^1\Pi_{1g}$ state vary between 1.9 and 8.3 cm^{-1}. These values are consistent with those observed ($\sim$6 cm^{-1}) in the spectra in Fig. 3, although the spectral quality was not high enough to observe any oscillation in the values $v=1$ of the $4s\,^3\Pi_{1g}$ state is anomalously sharp possibly because it interacts heterogeneously with the close lying $3d\,^3\Sigma^-_{0g}$ state as discussed in a previous study.[7]

It was predicted that the linewidths of $v=0$ and 1 of the $5s$ cluster should be less than 1 cm^{-1}. This is consistent with our observed values of $\sim$2 cm^{-1} which probably includes a small amount of power broadening. Similar narrow linewidths are observed for the higher-ns states, and this explains the relative ease with which they are seen, especially compared to the $4s$ states.

The same dissociation path is also available to the $nd\,^1\Pi_{1g}$ states and may, at least partially, explain why these have not been observed in two-photon spectra from the $X\,^3\Sigma^-_g$ and $a\,^1\Delta_{2g}$ states. This is especially true of the $3d$ cluster, which is nearly isoenergetic with the heavily predissociated $4s$ cluster. From comparison with the higher-ns clusters, it might be expected that some of the higher-$nd\,^1\Pi_{1g}$ states would be much less predissociated. It is believed that some of the unassigned lines, mentioned in Sec. III D above, are due to transitions to $nd\,^1\Pi_{1g}$ states. Thus the irregular intensities could indicate a vibrationally dependent degree of predissociation as predicted,[9] for instance, for the $4s\,^3\Pi_g$ state.

IV. CONCLUSIONS

Several $ns\,(n=4-9)$ and $nd\,(n=3-8)$ Rydberg states of O_2 have been observed using optical–optical double resonance with resonance-enhanced multiphoton ionization, excited via single-rotational levels of the $b\,^1\Sigma^+_{0g}$ valence state. Both ns and nd states show a transition from (Λ,S) coupling to (Ω,ω) coupling as n increases.

Transitions to all four components of an ns complex are observed as a result of the increased importance of spin–orbit coupling in the core and possibly S-uncoupling interactions as n increases. Rotational line strengths show that the $^3\Pi_{2g}\leftarrow\leftarrow b\,^1\Sigma^+_{0g}$ transition borrows intensity from the $^1\Pi_{1g}\leftarrow\leftarrow b\,^1\Sigma^+_{0g}$ transition and that the rotational line strengths are determined by those of the state that carries the oscillator strength.

ACKNOWLEDGMENT

The authors would like to thank Professor M. L. Ginter for detailed comments on the manuscript.

[1] A. Sur, C. V. Ramana, and S. D. Colson, J. Chem. Phys. **83**, 904 (1985).
[2] A. Sur, C. V. Ramana, W. A. Chupka, and S. D. Colson, J. Chem. Phys. **84**, 69 (1986).
[3] A. Sur, R. S. Friedman, and P. J. Miller, J. Chem. Phys. **94**, 1705 (1991).
[4] R. Ogorzalek-Loo, W. J. Marinelli, P. L. Houston, S. Arepalli, J. R. Wiesenfeld, and R. W. Field, J. Chem. Phys. **91**, 5185 (1989).
[5] A. Sur, L. Nguyen, and N. Nikoi, J. Chem. Phys. **96**, 6791 (1992).
[6] R. D. Johnson III, G. R. Long, and J. W. Hudgens, J. Chem. Phys. **87**, 1977 (1987).
[7] R. J. Yokelson, R. J. Lipert, and W. A. Chupka, J. Chem. Phys. **97**, 6153 (1992).
[8] Y. Wang, C. A. Woodward, and W. A. Chupka (unpublished).
[9] J. S. Morrill, M. L. Ginter, B. R. Lewis, and S. T. Gibson, J. Chem. Phys. **111**, 173 (1999).
[10] J. S. Morrill, Ph.D. thesis, University of Maryland, 1999.
[11] S. T. Pratt, J. L. Dehmer, and P. M. Dehmer, J. Chem. Phys. **93**, 3072 (1990).
[12] P. O'Keeffe, T. Ridley, K. P. Lawley, R. J. Donovan, H. H. Telle, D. C. S. Beddows, and A. G. Urena, J. Chem. Phys. **113**, 2182 (2000).
[13] T. Ridley, K. P. Lawley, H. A. Sheard, and R. J. Donovan, J. Chem. Phys. **116**, 451 (2002).
[14] P. O'Keeffe, T. Ridley, H. A. Sheard, K. P. Lawley, R. J. Donovan, and B. R. Lewis, J. Chem. Phys. **117**, 8705 (2002).
[15] A. M. Sjödin, K. P. Lawley, T. Ridley, H. A. Sheard, and R. J. Donovan, J. Chem. Phys. **118**, 8791 (2003) (following paper).
[16] W. L. Glab, P. M. Dehmer, and J. L. Dehmer, J. Chem. Phys. **104**, 4937 (1996).
[17] H. Park, L. Li, W. A. Chupka, and H. Lefebvre-Brion, J. Chem. Phys. **92**, 5835 (1990).
[18] R. G. Tonkyn, J. W. Winniczek, and M. G. White, Chem. Phys. Lett. **164**, 137 (1989).
[19] H. Park, P. J. Miller, W. A. Chupka, and S. D. Colson, J. Chem. Phys. **89**, 6676 (1988).
[20] H. Park, L. Li, and W. A. Chupka, Chem. Phys. Lett. **162**, 317 (1989).
[21] H. Park, L. Li, and W. A. Chupka, J. Chem. Phys. **92**, 61 (1990).
[22] R. J. Yokelson, R. J. Lipert, and W. A. Chupka, J. Chem. Phys. **97**, 6144 (1992).
[23] E. A. Colbourn and A. E. Douglas, J. Mol. Spectrosc. **65**, 332 (1977).
[24] T. G. Slanger and P. C. Cosby, J. Phys. Chem. **92**, 267 (1988).
[25] R. J. Yokelson, Y. Wang, C. A. Woodward, and W. A. Chupka (unpublished).
[26] R. G. Bray and R. M. Hochstrasser, Mol. Phys. **31**, 1199 (1976).
[27] B. R. Lewis, S. T. Gibson, J. S. Morrill, and M. L. Ginter, J. Chem. Phys. **111**, 186 (1999).
[28] P. J. H. Tjossem and K. C. Smyth, Chem. Phys. Lett. **144**, 51 (1988).
[29] W. J. van der Zande, W. Koot, J. Los, and J. R. Peterson, J. Chem. Phys. **89**, 6758 (1988).
[30] W. J. van der Zande, W. Koot, and J. Los, J. Chem. Phys. **91**, 4597 (1989).